Cell, Vol. 113, 195–206, April 18, 2003, Copyright ©2003 by Cell Press

The Conserved Nup107-160 Complex Is Critical for Nuclear Pore Complex Assembly

Tobias C. Walther,[1,4] Annabelle Alves,[2,4] Helen Pickersgill,[3,5] Isabelle Loïodice,[2] Martin Hetzer,[1] Vincent Galy,[1] Bastian B. Hülsmann,[1] Thomas Köcher,[1] Matthias Wilm,[1] Terry Allen,[3] Iain W. Mattaj,[1,4,*] and Valérie Doye[2,4]

[1]EMBL
Meyerhofstrasse 1
69117 Heidelberg
Germany

[2]UMR 144 CNRS-Institut Curie
26 Rue d'Ulm
75248 Paris Cedex 05
France

[3]CRC Department of Structural Cell Biology
Paterson Institute for Cancer Research
Christie Hospital National Health Service Trust
Manchester M20 9BX
United Kingdom

Summary

Nuclear pore complexes (NPCs) are large multiprotein assemblies that allow traffic between the cytoplasm and the nucleus. During mitosis in higher eukaryotes, the Nuclear Envelope (NE) breaks down and NPCs disassemble. How NPCs reassemble and incorporate into the NE upon mitotic exit is poorly understood. We demonstrate a function for the conserved Nup107-160 complex in this process. Partial in vivo depletion of Nup133 or Nup107 via RNAi in HeLa cells resulted in reduced levels of multiple nucleoporins and decreased NPC density in the NE. Immunodepletion of the entire Nup107-160 complex from in vitro nuclear assembly reactions produced nuclei with a continuous NE but no NPCs. This phenotype was reversible only if Nup107-160 complex was readded before closed NE formation. Depletion also prevented association of FG-repeat nucleoporins with chromatin. We propose a stepwise model in which postmitotic NPC assembly initiates on chromatin via early recruitment of the Nup107-160 complex.

Introduction

The existence of the nuclear envelope (NE) and the consequent compartmentalization of nucleic acid (DNA and RNA) and protein synthesis in eukaryotic cells generates a requirement for high-capacity macromolecular transport between the nucleus and the cytoplasm. Nucleocytoplasmic transport involves active, receptor-mediated translocation through nuclear pore complexes (NPCs) (Conti and Izaurralde, 2001; Görlich and Kutay, 1999; Mattaj and Englmeier, 1998). These structures fuse the two lipid bilayers of the NE, the inner and outer nuclear membranes (INM, ONM), and form aqueous channels (Doye and Hurt, 1997; Vasu and Forbes, 2001).

NPCs have a modular architecture (Bagley et al., 2000; Stoffler et al., 1999). Substructures include an 8-fold symmetric spoke-ring complex anchored in the NE, cytoplasmic and nuclear annular rings, and, at least in metazoa, asymmetric cytoplasmic and nuclear filamentous structures. Both yeast and human NPCs have recently been shown to consist of roughly 30 nucleoporins that are present either in eight copies per NPC or in multiples of eight (Allen et al., 2001; Cronshaw et al., 2002; Rout et al., 2000).

Genetic and biochemical studies, mostly of the yeast *S. cerevisiae*, have identified groups of nucleoporins that are tightly associated and that may correspond to NPC modules (Doye and Hurt, 1997; Ohno et al., 1998; Vasu and Forbes, 2001). Components of these different modules are sequentially recruited to the reassembling NE late in metazoan mitosis, suggesting that NPC assembly is an ordered process (Belgareh et al., 2001; Bodoor et al., 1999; Daigle et al., 2001; Haraguchi et al., 2000). Nucleoporins are generally not well conserved in evolution (Ohno et al., 1998; Vasu and Forbes, 2001), but those that are more conserved include the components of the *S. cerevisiae* scNup84 complex. scNup84 is the homolog of rat Nup107 (Radu et al., 1994) and purifies in a complex consisting of scNup85, scNup120, scNup145-C, scSeh1 (Sec 13 homolog 1), and scSec13 (Siniossoglou et al., 1996, 2000). scNup84 also interacts directly with scNup133 (Belgareh et al., 2001). A complex of these seven nucleoporins has been reconstituted from recombinant components (Lutzmann et al., 2002).

Mutation of scNup84 complex components leads to a variety of phenotypes that include nuclear polyA$^+$ RNA accumulation, NPC clustering in the NE, and abnormalities in NE organization (Doye and Hurt, 1997). Analysis of vertebrate nucleoporins points to the conclusion that at least 5 of the equivalent proteins: Nup107, Nup133, Nup96 (homologous to scNup145-C), Nup160/Nup120, and Sec13 form an analogous complex that we will refer to as the Nup107-160 complex (Belgareh et al., 2001; Fontoura et al., 1999; Vasu et al., 2001). Both the yeast and human complexes appear to be located symmetrically on both sides of the NE (Belgareh et al., 2001; Rout et al., 2000). Overexpression of fragments of Nup160 and Nup133 led to nuclear polyA$^+$ RNA accumulation (Vasu et al., 2001) providing a first indication for functional conservation of the complex.

Additional information on the complex came from an analysis of the localization and dynamics of Nup133 and Nup107 in mammalian cells (Belgareh et al., 2001). Aside from the unexpected observation that a small fraction of each protein was kinetochore-associated during mitosis two other results were of particular interest. First, unlike other previously studied nucleoporins that showed very rapid exchange at the NPC during interphase, like Nup153 and gp210 (Daigle et al., 2001; G. Rabut and J. Ellenberg, personal communication), Nup133 and Nup107 were both immobile NPC components that moved on

*Correspondence: mattaj@embl-heidelberg.de

[4]These authors contributed equally to this work.

[5]Present address: Netherlands Cancer Institute, H4, Plesmanlaan 121, 1066 CX Amsterdam, Netherlands

or off the NPC roughly once per cell cycle. Second, the two proteins accumulated at the reforming NE at the end of mitosis earlier than other nucleoporins whose behavior in this regard has been studied (Belgareh et al., 2001, and references therein). Given the biochemical data reviewed above and subsequent analysis of the dynamics of four known Nup107-160 complex components (G. Rabut and J. Ellenberg, personal communication), it now seems that the whole complex behaves similarly. These observations suggested that the Nup107-160 complex might have an early role in NPC assembly and, once incorporated, be a stable anchoring point for other, more mobile, Nups. The data reported here provide strong support for this hypothesis and demonstrate a critical role for the Nup107-160 complex in postmitotic NPC formation.

Results

In Vivo Depletion of Nup133 or Nup107 Reduces NPC Density in the NE

The function of the Nup107-160 complex was first addressed using RNA interference. Small interfering (si) RNA duplexes (Elbashir et al., 2001) targeted to Nup133 or Nup107 were transfected into HeLa cells and the effects on both their targets and other nucleoporins were assayed. In most Nup133 siRNA-treated cells, presumably those transfected, immunofluorescence analysis revealed a gradual reduction of Nup133 staining at the NE over 3 days, consistent with the gradual loss of this stable protein by dilution as the cells underwent division (Figure 1A, D1–D3). A similar reduction in Nup107 immunofluorescence was seen in Nup107 siRNA-treated cells (Figure 1B). Unexpectedly, in both cases a progressive but less severe reduction of NE staining was seen using the mAb414 antibody, that recognizes a group of FG-repeat containing nucleoporins (Davis and Blobel, 1986; Figures 1A and 1B). In most Nup133-depleted cells and some Nup107-depleted cells, a transient increase in cytoplasmic foci that contained mAb414 antigens, Nup133, and Nup107 was also observed (Figures 1A, 1B, 2A, and Supplemental Figure S1A available at http://www.cell.com/cgi/content/full/113/2/195/DC1). Thin section EM analysis revealed frequent annulate lamellae (AL) in the Nup133 siRNA-treated cell population (Figure 1C). Since no such structures were detected in nontransfected control HeLa cells of the same strain (data not shown), this indicates that the cytoplasmic foci are probably AL (see Discussion).

To determine how the total cellular levels of various Nups were affected by the depletions, Western blot analysis of cells transfected with Nup133, Nup107, or control siRNAs was made 3 days after transfection. The data were quantified by comparing Western blots of dilutions of control and depleted cell extracts (data not shown). An unspecific crossreacting band (asterisk) and protein staining act as loading controls. The level of Nup133 remaining in Nup133 siRNA-treated cells, corrected for the transfection efficiency of 90%, was in the range of 15%–20% (Figure 1D). Surprisingly, the levels of several nucleoporins were reduced by at least 50%. These included Nup107 and Nup96 that are both components of the Nup107-160 complex, Tpr and Nup153. In contrast, no decrease in p62 or gp210 was observed (Figure 1D). Nup107 siRNA treatment caused similar reductions in the levels of these nucleoporins.

To further investigate the effects of Nup107 and Nup133 depletion on the distribution of other Nups, a series of immunolocalizations was carried out with Nup107, Nup133, or mAb414 counterstaining. Control cells and cells after 3 days of Nup107 siRNA treatment are shown in Figure 2A; for Nup133 depletions, see Supplemental Figure S1A available at http://www.cell.com/cgi/content/full/113/2/195/DC1. There was a considerable reduction in nuclear rim staining of Nup133 (Figure 2A; a, a′), Nup96 (Figure 2A; b, b′), Nup98 (Figure 2A; c, c′), Tpr (Figure 2A; d, d′), Nup93, p62, CAN/Nup214, and RANBP2/Nup358 (data not shown). gp210 and Nup153 (Figure 2A; e, e′, f, f′) also showed reduced staining at the NE but in these cases the extent of reduction was variable and for Nup153 was less. Lamin A/C staining (Figure 2A; g, g′) was not affected. All of the nucleoporins except Nup153 transiently colocalized with mAb414 to the AL-like cytoplasmic foci, as best seen in the Nup133-depleted cells (Figures 1A and Supplemental Figure S1A available at above website). In the case of Nup153, but not of any of the other nucleoporins tested, evidence for some aggregation in the plane of the NE was observed in a subset of cells (e.g., Figure 2A, f). Tpr initially delocalized throughout the nucleus and, to a minor extent, to the mAb414-labeled cytoplasmic foci. Later, Tpr relocalized to bigger cytoplasmic and nuclear aggregates which did not contain other nucleoporins (Figure 2A; d, d′, Supplemental Figure S1A available at above website).

We next examined effects on nucleocytoplasmic transport. While the basic NLS-containing lamin proteins localized normally (Figure 2A, g) and import of an RGG reporter protein was unaffected (data not shown), nuclear accumulation of poly A^+ RNA was observed in Nup107 (Figure 2B) and Nup133 (Supplemental Figure S1B available at above website) siRNA-treated cells. Both SC-35 (Figure 2B and Supplemental Figure S1B available at above website) and PML (data not shown) relocalized from the nucleus to cytoplasmic aggregates, distinct from AL or Tpr foci, in some Nup107 and Nup133 siRNA-treated cells, possibly reflecting an effect on the nucleocytoplasmic transport of these proteins.

The above results indicated that NPC assembly might be impaired by depletion of Nup107 or Nup133. Field emission in-line scanning electron microscopy (FEISEM) of cells treated to expose the nuclear surface (Allen et al., 1998) was used to further examine this possibility. The density of NPCs per unit area was much lower in the Nup133 siRNA-treated cells than in control cells (Figure 2C). Quantitation of NPC density in control NEs gave a mean value of 24 NPCs μm^{-2}, the median range being in the 20–24 μm^{-2} interval. In Nup133-depleted cells, the mean density was 8.5 NPCs μm^{-2} and the median value was in the 4–8 μm^{-2} range. At this level of resolution, some remaining NPCs had an abnormal surface appearance while others did not (Figure 2C).

Nup107 and Nup133 Associate with Chromatin Early during Nuclear Assembly In Vitro

The in vivo data strongly suggested a function for Nup133 and Nup107, and thus the Nup107-160 complex,

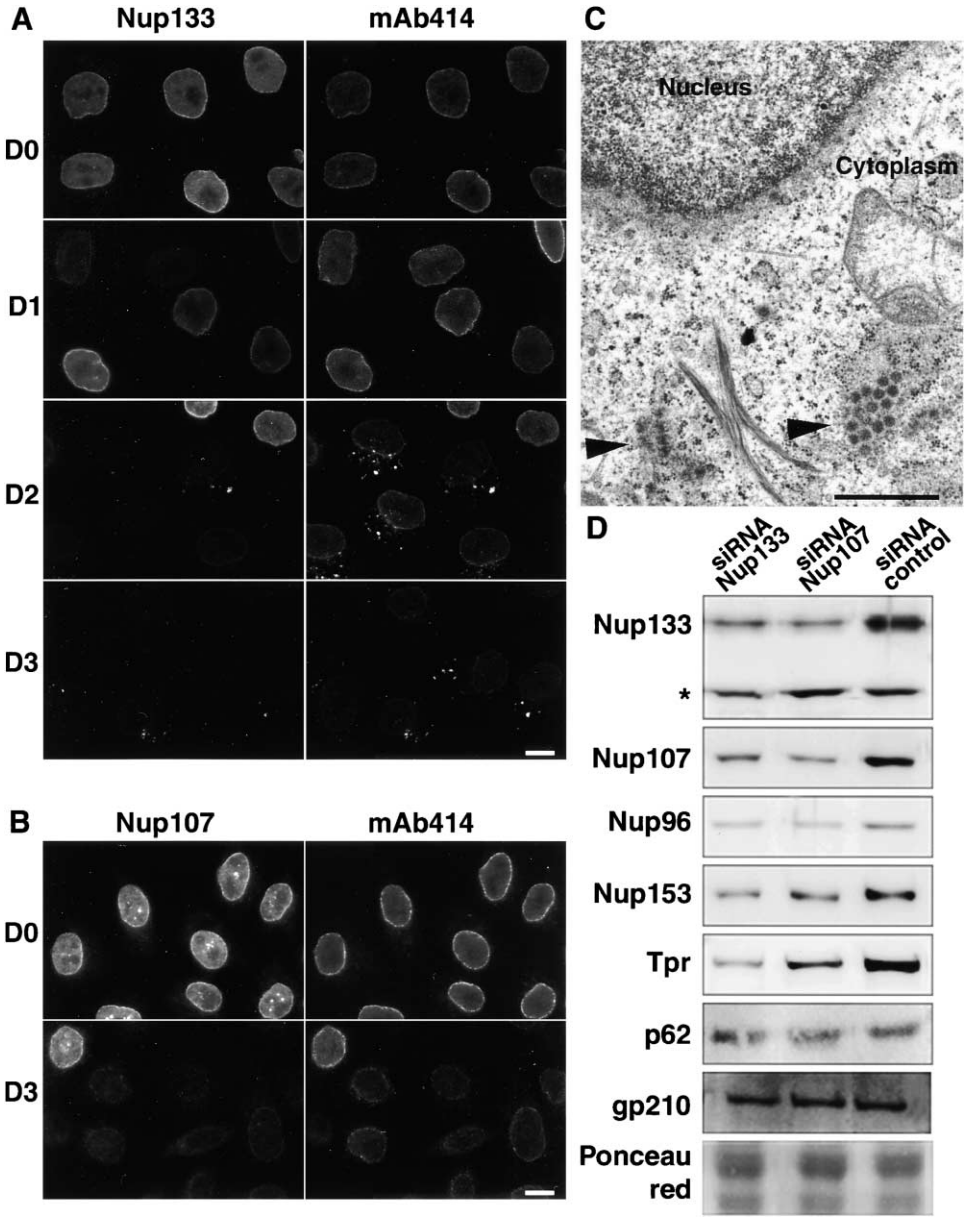

Figure 1. Depletion of Nup133 and Nup107 Results in Reduced Cellular and NE Levels of Various Nucleoporins

(A and B) HeLa cells transfected with siRNA duplexes specific for Nup133 (A) or Nup107 (B) were fixed after 24 (D1), 48 (D2), or 72 (D3) hr and analyzed by immunofluorescence microscopy using affinity-purified anti-Nup133 or Nup107 antibodies in combination with mAb414. Mock-treated cells (D0) are shown as control. Bar is equal to 10 μm.

(C) Thin section EM of HeLa cells fixed after 3 days of Nup133 siRNA treatment show annulate lamellae (arrows) in the cytoplasm. Bar is equal to 1 μm.

(D) Whole-cell extracts from Nup133, Nup107, or control siRNA-treated HeLa cells were made 3 days after transfection and analyzed by Western blot using the antibodies indicated on the left. An unspecific crossreacting band (*) and Ponceau red staining are shown as loading controls.

in NPC assembly. However, the general reduction in the level of most nucleoporins examined in the depleted cells and the effects on nucleocytoplasmic transport made it essential to employ a more direct approach to test the function of the Nup107-160 complex. An in vitro system based on *Xenopus* egg extract, which recapitulates pronuclear assembly and mimics the events of postmitotic NE reassembly was therefore used (Forbes et al., 1983; Lohka and Masui, 1983; Newport, 1987). Previously such reactions have been used to assay the effects of immunodepletion of several nucleoporins (Finlay and Forbes, 1990; Finlay et al., 1991; Grandi et al., 1997; Powers et al., 1997; Walther et al., 2001, 2002).

We first determined whether components of the Nup107-160 complex are incorporated early during NE reassembly, as in mammalian cells. A time course of immunofluorescence staining on sperm chromatin that acts as a template for nuclear assembly was carried out.

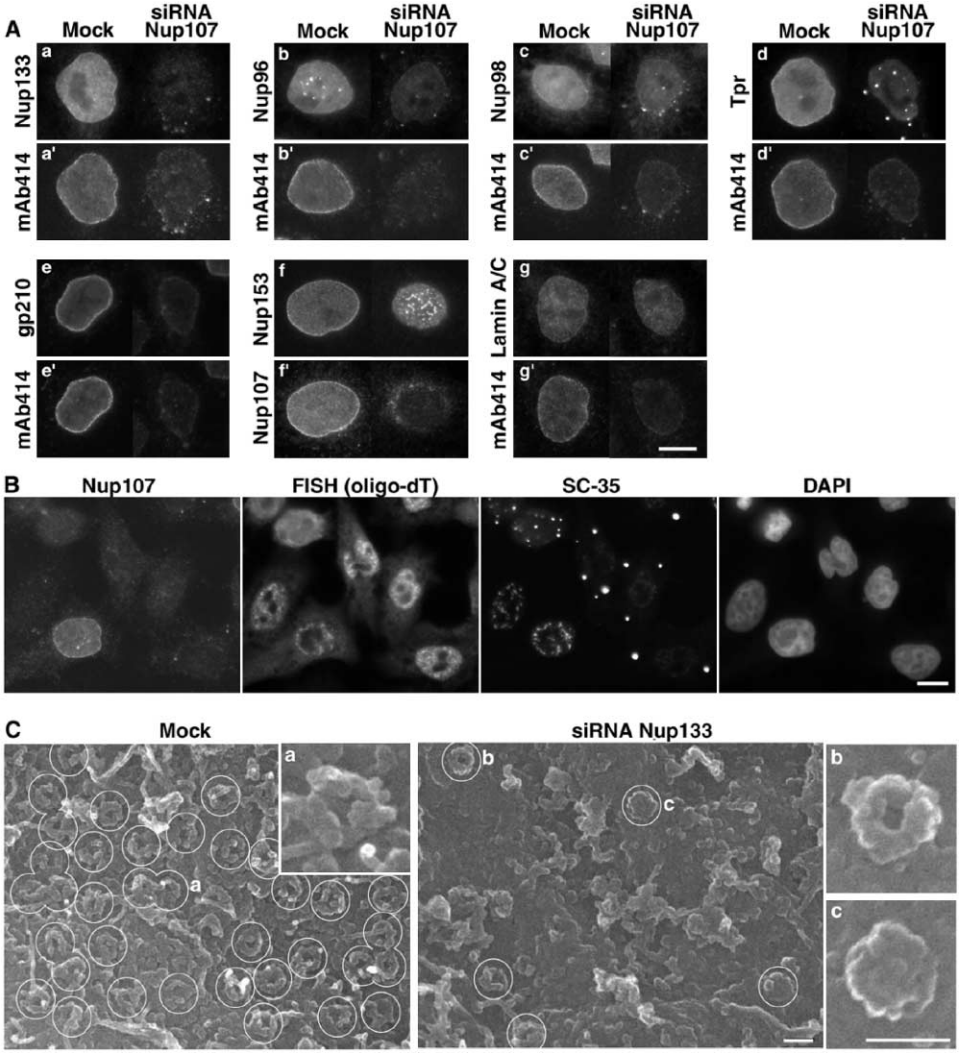

Figure 2. Fluorescence and FEISEM Analysis of Nup107 and Nup133-Depleted HeLa Cells

(A) Widefield microscopy images of immunofluorescence of nontransfected cells (left) and cells treated for 3 days with Nup107 siRNA (right) with anti-Nup133 (a), Nup96 (b), Nup98 (c), Tpr (d), gp210 (e), Nup153 (f), or lamin A/C (g) antibodies with either mAb414 or Nup107 counterstaining as indicated (a′–g′). For Nup153, a tangential section (f, f′) that reveals its partial aggregation is shown. Bar is equal to 10 μm.

(B) Nup107-depleted cells were analyzed by FISH using Cy3-labeled oligo-dT and immunofluorescence with anti-Nup107 and anti-SC-35 antibodies as indicated. DNA was stained with DAPI. Bar is equal to 10 μm.

(C) FEISEM analysis of the NE surface of (a) mock- or (b) Nup133 siRNA-treated HeLa cells. NPCs are circled. Insets show enlargement of marked NPCs. Bars are equal to 100 nm.

Both Nup107 and Nup133 associated with the chromatin surface early by comparison with the group of Nups recognized by mAb414 (Figure 3). By 10 min, a general, somewhat punctate staining of both Nup107 and Nup133 was seen. This chromatin staining occurred before addition of membrane fractions, i.e., in the absence of NE assembly (see also Figure 7A below). As the nuclear assembly reaction progressed, a further difference was observed. Both Nup107 and Nup133 staining covered the entire chromatin surface at intermediate assembly times, while mAb414 staining remained punctate throughout (Figure 3, mb+30 min images). In the presence of membrane fractions, reactions proceeded to complete nuclear assembly (lowest images).

Nup107 and Nup133 appeared to be colocalized at all time points (inset images). Their identical behavior probably means that the entire Nup107-160 complex binds early to chromatin. As shown below, all the Nup133 in the extract is associated with Nup107, further supporting this assumption, but reagents against other complex components that would be required for definitive proof are currently unavailable.

Depletion of Nup107 Blocks NPC Insertion into the NE In Vitro

The effect of Nup107 depletion on NE assembly was tested. Affinity-purified antibodies were immobilized and egg extract was passed over them. After two rounds of depletion, both Nup107 and Nup133 had been effectively removed from the extract (Figure 4A). All detectable Nup133 was codepleted with Nup107, demonstrating that Nup133 is quantitatively in a complex with

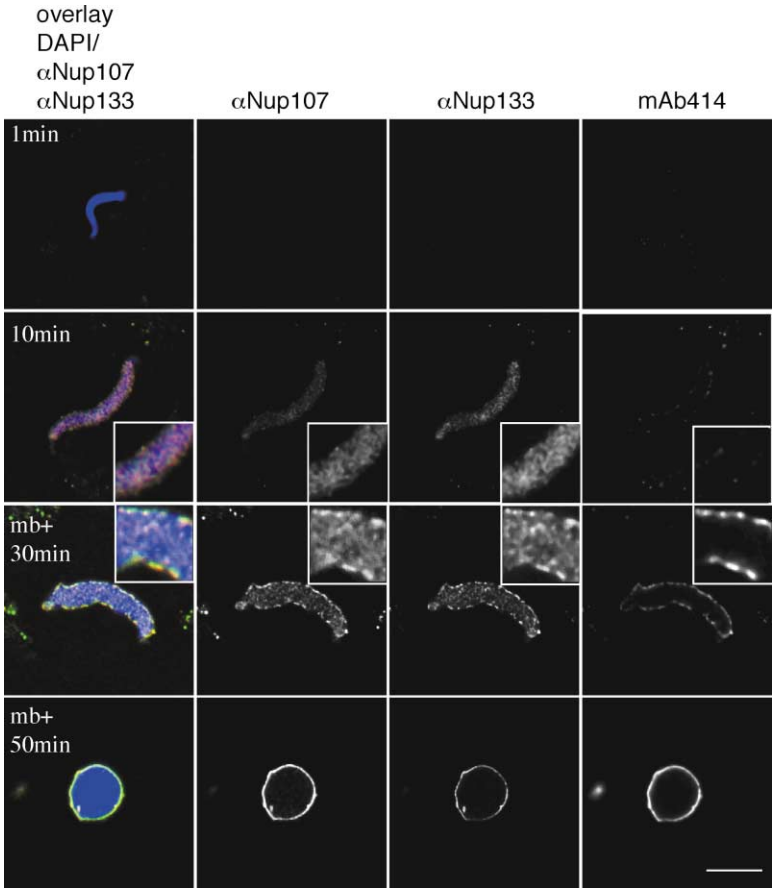

Figure 3. Time Course of Nucleoporin Recruitment to Chromatin in a Nuclear Reconstitution Assay

Demembranated sperm chromatin was incubated in *Xenopus* egg extract. After 10 min, membranes (mb) were added to the reaction. A sample was removed from the reaction at the indicated time points and analyzed by confocal microscopy after immunofluorescence using anti-Nup107 (green in the overlay), biotinylated anti-Nup133 (red in the overlay), and mAb414. Chromatin was stained with DAPI (blue in the overlay). Insets are higher magnifications. Bar is equal to 10 μm.

Nup107. Interestingly, a higher proportion of Nup107 than of Nup133 was removed after the first depletion, indicating that some Nup107 is present in a Nup133-free form (Figure 4A, top images). It should be noted that only a minor phenotype was associated with a single round of depletion even though much of the Nup107 was removed at this step. More complete removal of Nup107 and the consequent efficient depletion of Nup133 (and most likely other constituents of the 107-160 complex) were required to observe the strong phenotype described below.

The effect of depletion on nuclear assembly was first tested using fluorescently labeled membrane fractions (Hetzer et al., 2000) and observing nonfixed samples directly in the confocal microscope. Fixed samples were then analyzed in conjunction with NPC immunofluorescence analysis. In order to rule out effects due to nuclear or NE growth, relatively early assembly times (60–90 min) were recorded, although the differences described below persisted at later times. This meant that many of the nuclei were irregular in shape (Figure 4B).

In Nup107-depleted extracts, closed NEs were formed on chromatin templates at an efficiency similar to that observed in the mock-depleted controls (Figure 4B, top images). The other membrane structures seen in these two images are a mixture of aggregated membrane vesicles and assembling endoplasmic reticulum (Hetzer et al., 2001). In contrast, no mAb414 rim fluorescence was detected on nuclei assembled in Nup107-depleted extract although strong staining was seen in mock-depleted reactions (Figure 4B, lower images). To examine this in more detail, the NE surface was visualized by FEISEM. Whereas very abundant NPC structures were seen in the NEs of nuclei assembled for either 30 or 90 min in mock-depleted extract (Figure 4C), essentially no NPCs were seen on nuclei assembled in Nup107-depleted extract (Figure 4D). The density of NPCs after 90 min of assembly fell from $20 \pm 1.8\ \mu m^{-2}$ to $0.008 \pm 0.008\ \mu m^{-2}$. In addition, none of the intermediates in NPC assembly (dimples, pores, star-rings, and thin rings; Goldberg et al., 1997) were detected. This suggested that Nup107, as part of the Nup107-160 complex, plays a critical role in postmitotic NPC assembly in the NE.

Purified Nup107-160 Complex Restores NPC Assembly and Function

To prove that the effect of depletion was a specific result of removal of the Nup107-160 complex, it was necessary to complement the defect. The Nup107-160 complex was purified from *Xenopus* egg extract using short fragments of both Nup153 and Nup98 that had previously been used in affinity enrichment of the complex (Vasu et al., 2001). Similar fragments to those of Vasu et al., as well as a control fragment from CAN/Nup214 (Figure 5A), were fused to the TAP tag (Rigaut et al., 1999) and used for purification. As previously observed (Vasu et al., 2001), four prominent common bands were seen in both Nup98 and Nup153 eluates (Figure 5B, compare

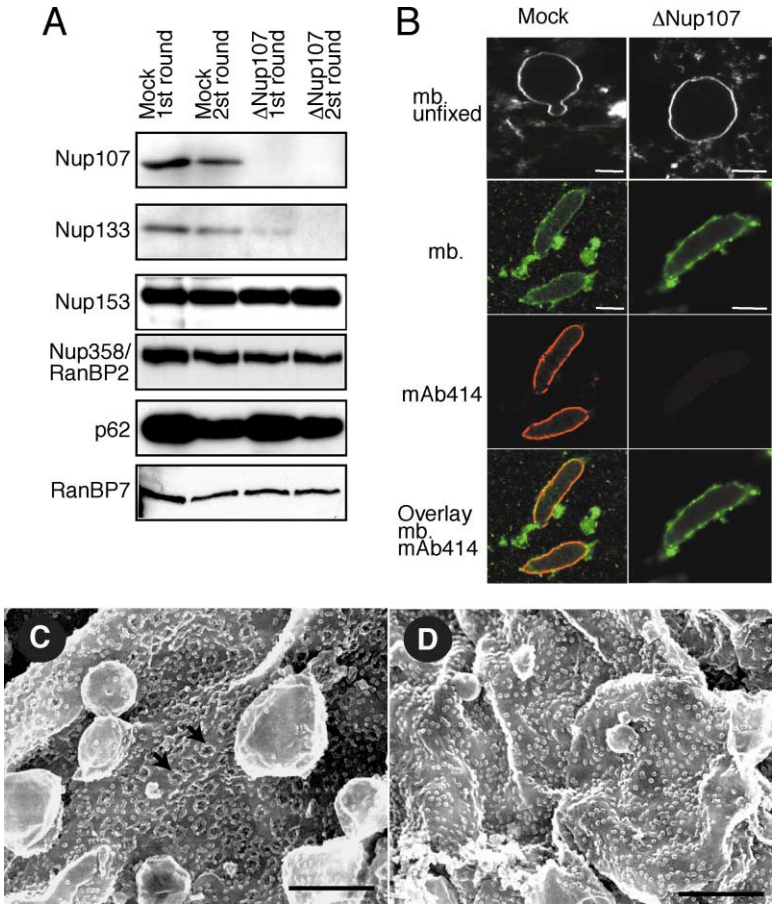

Figure 4. Nuclei Formed in Nup107 Depleted Lack NPCs

Nup107 was depleted from the *Xenopus* nuclear reconstitution system by two rounds of incubation with immobilized anti-Nup107 antibodies.

(A) Western blot analysis of mock and Nup107-depleted extracts using the antibodies indicated on the left.

(B) Nup107- or mock-depleted nuclei support NE assembly around chromatin. Nuclei were assembled for 2 hr in the presence of prelabeled (DiIC6) membranes. Samples were removed and analyzed unfixed by confocal microscopy (top images). Other samples were fixed and membrane stain and immunofluorescence with mAb414 (red) were analyzed by confocal microscopy. Overlay of the membrane and antibody signals is also shown. The disordered NE membrane "aggregation" phenotype seen in these samples is caused by fixation. Bars are equal to 10 μm.

(C and D) Nuclei were assembled for 90 min in either mock (C) or Nup107-depleted extracts (D) and processed for FEISEM. Representative images of the nuclear surfaces are shown. Bar is equal to 500 nm.

CAN/Nup214 control lane with the experimental lanes). Confirmation of the presence of Nup133 and Nup107 in the eluted fractions and of their different concentrations in the two fractions was obtained by Western blot (Figure 5C). Mass spectrometric analysis of the major bands led to detection of Nup107 and Nup133 and to the identification of Nup160 and Nup96 in both the Nup98 and Nup153 eluates, as well as of RanBP7 and importin β in the Nup153 eluate. The interaction of the two import receptors with the Nup153 column did not depend on their association with the Nup107-160 complex (data not shown).

The two purified complex fractions and the control eluate were then used in addback experiments. None of these fractions had any effect when added to mock-depleted extract (data not shown). In addition, the CAN eluate had no effect on Nup107 or mAb414 staining of nuclei assembled in depleted extract (Figure 6A, middle images). Addition of the Nup98 eluate resulted in significant, but weak, restoration of both the Nup107 and mAb414 rim fluorescence (Supplemental Figure S2 available at http://www.cell.com/cgi/content/full/113/2/195/DC1). The more concentrated Nup153 eluate (Figure 5B) resulted in further enhanced rim fluorescence of both antigens (Supplemental Figure S2 available at above website). The best complementation was however consistently obtained when a 1:1 mix of both eluates, that contains less Nup107-160 complex than the undiluted Nup153 eluate, was used (Figure 6A). Immunofluorescence analysis of these nuclei revealed discontinuities in NPC staining in the plane of the NE indicating that NPC assembly was not restored to wild-type levels. Adding the purified complexes, however, only restored Nup107 and Nup133 levels to maximally 50% of those in control extract, as determined by Western blot comparison of dilutions of undepleted extract and of the purified complex fractions (data not shown).

While both Lamin LIII and Nup153 immunofluorescence was undetectable in nuclei assembled in Nup107-depleted extracts, complementation restored both antigens to the nuclear rim (Figure 6A, lower images). The difference in Lamin and Nup153 accumulation seen when the in vivo and in vitro depletion experiments are compared (Figures 2 and 6) is most likely related to the fact that NPCs were essentially undetectable in the in vitro case whereas they were still present, although at a reduced level, after in vivo depletion.

When NPC function in nuclear protein import was assayed, using a GFP-NLS fusion protein as substrate, the results qualitatively reflected the restoration of Nup107 and mAb414 antigen presence at the nuclear rim (Figure 6B). GFP-NLS and a control, BSA-SLN (Palacios et al., 1997), were not detected above background in nuclei assembled in Nup107-depleted extract (Figure 6B and data not shown). Complementation with the Nup98 or Nup153 eluates partially restored GFP-NLS import and the mixed eluates resulted in restoration of import to a level that was not significantly different from that seen in mock-depleted extract (Figure 6B).

When closed NEs were allowed to reassemble prior

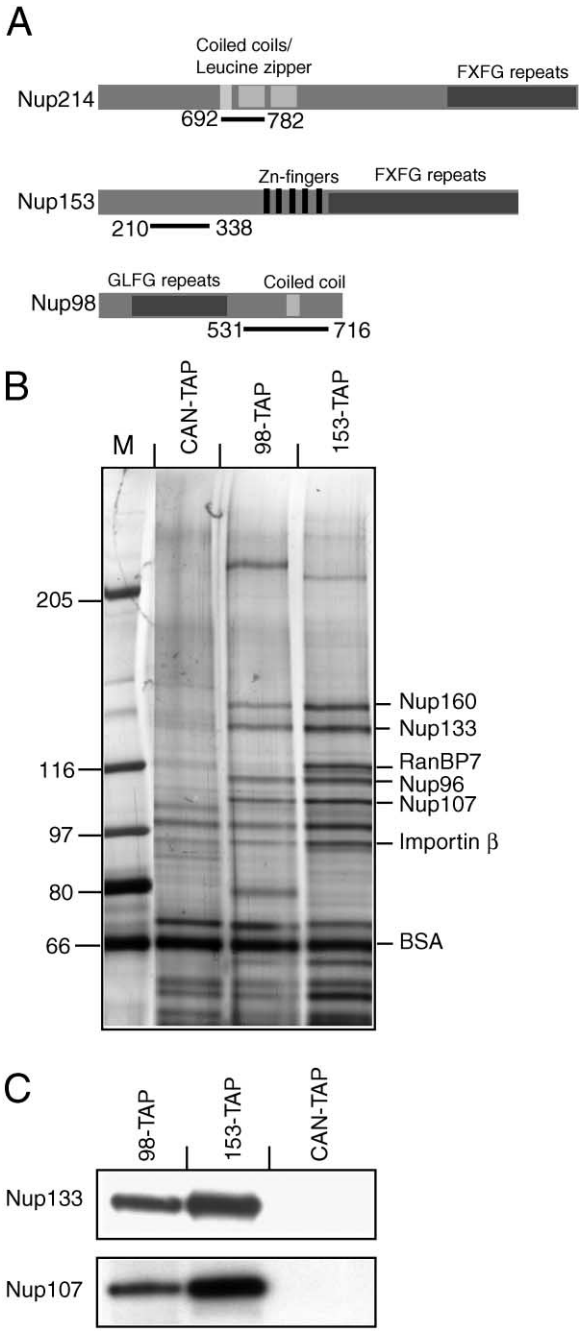

Figure 5. Purification of the Nup107-160 Complex

(A) Schematic representation of nucleoporin fragments used for affinity purification of the Nup107-160 complex. The full-length nucleoporins and some of their structural features are indicated by gray boxes. The segments fused to the TAP-tag are indicated below by black lines. Numbers represent amino acid positions within the protein.

(B) Silver-stained gel of proteins binding to TAP-tagged nucleoporin fragments. The bait fragments are indicated above the lane, the position of proteins identified by mass spectrometry is indicated on the right, and size markers are on the left.

(C) Western blot analysis of fractions like these in (B) using anti-Nup133 and anti-Nup107 antibodies as indicated.

to the addition of the purified Nup107-160 complex, no recruitment of mAb414 antigen to the NE was seen (data not shown). This suggested that the presence of Nup107-160 complex, on chromatin, prior to NE closure was essential for NPC assembly. To rule out that this result was simply due to insufficient Nup107-160 complex in the addback fractions, similar assembly experiments were performed, in which mock-depleted extract was added to the Nup107-depleted extract either before or after formation of a closed NE. As expected, when depleted and mock-depleted extracts were mixed at the beginning of the experiment, mAb414 antigens were efficiently incorporated into the NE (Figure 6C; fourth column). In contrast, when mock-depleted extract was added to preformed nuclei in Nup107-depleted extract, no significant mAb414 staining was observed (Figure 6C; third column). We conclude that the presence of the Nup107-160 complex is required prior to NE closure for postmitotic NPC assembly into the NE.

Depletion of Nup107 or BAPTA Treatment Prevents Stable Association of mAb414 Antigens with Chromatin

In order to gain more insight into the step at which NPC assembly is affected by removal of the Nup107-160 complex, we examined the accumulation kinetics of mAb414 antigens on chromatin. In contrast to the situation in mock-depleted extract, almost no mAb414 staining was seen on chromatin at any time in the reaction carried out in the Nup107-depleted extract (Figure 7A, the inset images are longer exposures). Chromatin decondensation and NE formation, in contrast, proceeded at similar rates in both cases (Figure 7A, Figure 4). In particular, no mAb414 labeling was observed at the 10 min time point, i.e., before the addition of membranes. This suggests that the removal of the Nup107-160 complex not only prevents assembly into NPCs of the group of nucleoporins recognized by mAb414, but also blocks an even earlier step in the recruitment of these proteins to the chromatin surface prior to their insertion into the NE.

To obtain further evidence for this mechanism of NPC insertion, we reinvestigated the point at which BAPTA, a calcium chelator previously shown to block NPC assembly in the NE (Macaulay and Forbes, 1996; Allen et al., 1998), inhibits NPC assembly into the NE. As expected from prior studies, EGTA had no effect on Nup107 or mAb414 recruitment to chromatin or their incorporation into a closed NE (Figure 7B, top). In contrast, BAPTA allowed formation of a closed NE and subsequent chromatin decondensation, but no NPCs were present, as seen by the lack of mAb414 antigens in the NE at the end of the assembly reaction (Figure 7B, right images, bottom row; see also Macaulay and Forbes, 1996; Allen et al., 1998). When recruitment of Nup107 and the mAb414 antigens was examined, Nup107 recruitment was seen to occur normally in a punctate pattern superimposed on general chromatin staining (Figure 7B, bottom, middle row). In contrast, mAb414 antigens never accumulated above background levels. This strongly suggests that BAPTA blocks a step in NPC assembly corresponding to the recruitment of FG repeat-containing nucleoporins to chromatin to which the Nup107-160 complex is bound, and that this step is critical for NPC assembly in the NE.

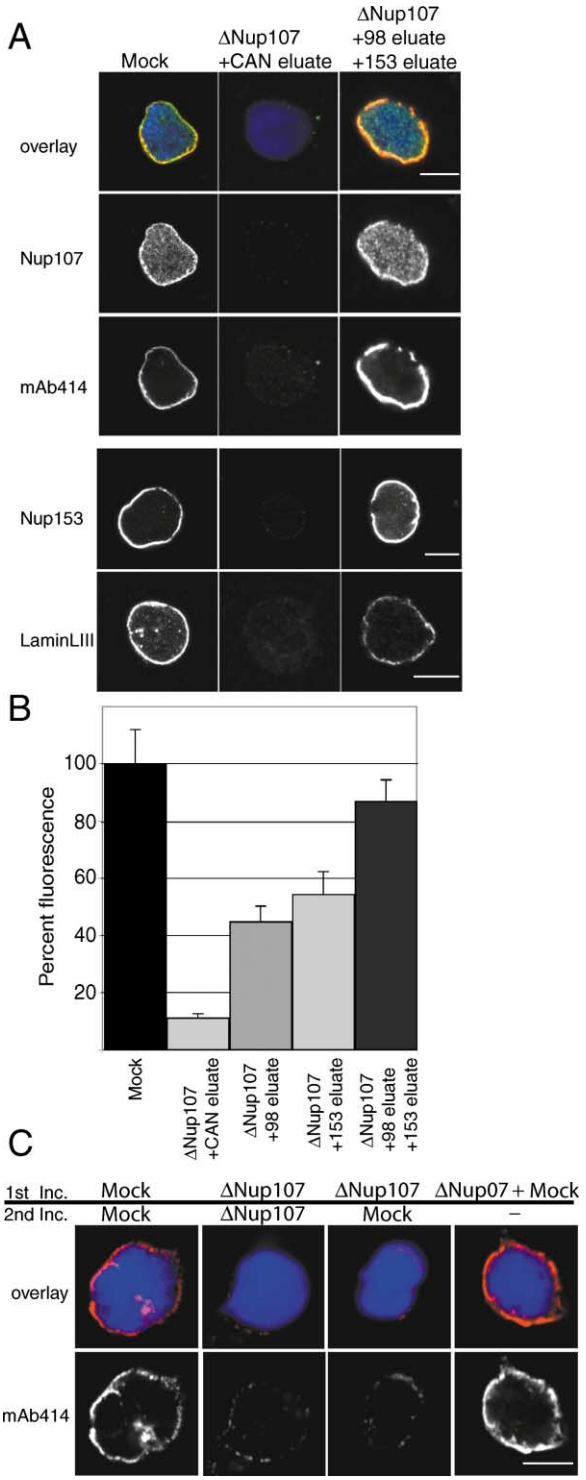

Figure 6. Addition of the Nup107-160 Complex Prior to NE Formation Restores NPC Assembly and Import Defect of Nuclei Assembled in Nup107-Depleted Extracts

Nup107-160 complex containing fractions purified on fragments of Nup98 or Nup153 or control fractions purified on a fragment of CAN/Nup214 were added to Nup107-160 complex depleted extracts and nuclei were assembled.

(A) Nuclei were fixed after 2 hr and immunofluorescence using anti-Nup107, mAb414, anti-Nup153, or S49 (anti-Lamin LIII) are shown. Scale bar is equal to 10 μm.

(B) After 2 hr, GFP-NLS import cargo was added to the assembled nuclei and the reactions were incubated for 30 min. After fixation, import was visualized by confocal microscopy. The GFP-NLS signal from multiple nuclei was quantified. Error bars represent standard errors between different nuclei.

(C) Chromatin templates decondensed in the presence of nucleoplasmin and core histones for 30 min (Hetzer et al., 2000) were added to mock-depleted or Nup107-depleted extract or a 1:1 mix of the two as indicated. Nuclear assembly was allowed to proceed for 90 min and NE integrity was checked. A second extract was added, as indicated above the figure, to a final ratio of 50% of the reaction volume and the reaction allowed to proceed for a further 60 min. Scale bar is equal to 10 μm.

Discussion

The effects of depletion of Nup107 and Nup133 have been examined both in vivo and in vitro. These two nucleoporins are components of an evolutionarily conserved complex called the Nup107-160 complex in vertebrates and the Nup84 complex in *S. cerevisiae*. In vivo depletion resulted in a complex phenotype. The major observation was a considerable reduction in NE-associated immunofluorescence signal for the targeted nucleoporin, other Nup107-160 complex components, and other nucleoporins not known to form any direct association with the Nup107-160 complex. FEISEM analysis of the depleted nuclei indicated that this loss of fluorescence resulted from a decreased NPC density within the NE. A second and possibly linked consequence of the loss of nucleoporins from the NE was a reduction in the total cellular level of several nucleoporins. Given the other data presented here, it seems likely that this loss is secondary to a defect in NPC assembly in the siRNA-treated cells and reflects the degradation of nucleoporins that are not incorporated into NPCs.

These phenotypes were accompanied, particularly in Nup133-depleted cells, by the transient relocation of part of the pool of many nucleoporins, including remaining Nup133 and Nup107, to cytoplasmic structures that were identified as annulate lamellae (AL) by thin section EM. AL are membrane stacks containing NPC-like structures that are found naturally in some cell types and whose production can be induced by imbalanced nucleoporin levels (Daigle et al., 2001; Imreh and Hallberg, 2000; Wu et al., 2001). A decrease in accumulation of several nucleoporins at the NE and the induction of AL production were also observed in Nup98$^{-/-}$ mouse cell lines (Wu et al., 2001). However, unlike Nup107 or Nup133 depletion, removal of Nup98 did not affect Nup96 or Nup93 targeting to the NE or the overall number of NPCs (Wu et al., 2001). Furthermore, depletion of Nup98 from in vitro assembled nuclei did not lead to a defect in NPC insertion (Powers et al., 1997). It therefore seems likely that the similarities are superficial and not a reflection of a similar mechanistic defect in cells lacking Nup98 and either Nup133 or Nup107. In addition, AL formation was not seen in vitro in the complete absence of the Nup107-160 complex (data not shown). We therefore suspect that the transient induction of AL formation in the siRNA-treated cells reflects defective NPC assembly due to unbalanced nucleoporin levels. Similarly, at least some of the effects of Nup133 or Nup107 depletion

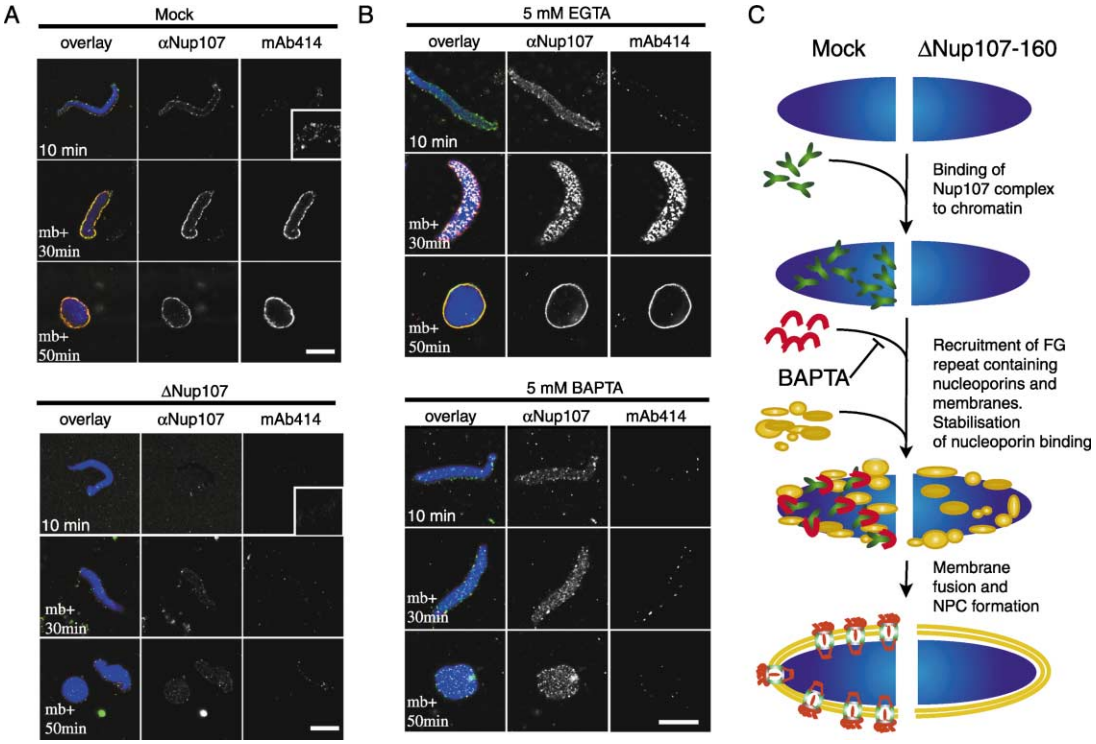

Figure 7. Depletion of Nup107 Prevents Stable Recruitment of mAb414 Reactive Nucleoporins to Chromatin

(A) A time course experiment was performed as in Figure 3. Time points before and after additions of membranes (mb) are shown. Insets are longer exposures of parts of the images at higher magnification. Bar is equal to 10 μm.

(B) Assembly reaction, as in (A) using non-depleted extract in the presence of 5 mM EGTA (left) or 5 mM BAPTA (right). Bar is equal to 10 μm.

(C) Model of the function of the Nup107 complex in NPC assembly. See text for details.

on nucleocytoplasmic transport may be secondary consequences of partial loss of other nucleoporins or reduction in NPC number.

Removal of the Nup107-160 Complex Prevents NPC Assembly

The in vivo depletion data were suggestive of an important role for the complex early in NPC assembly. Consistent with this possibility, when chromatin templates were added to Nup107-depleted *Xenopus* egg extract they were efficiently incorporated into closed NEs, but these NEs lacked detectable NPCs. Removal of Nup107 from the extracts by immunodepletion resulted in efficient codepletion of Nup133, suggesting that the entire Nup107-160 complex had been depleted. The defect in NPC assembly could be reversed with affinity-purified (Vasu et al., 2001) Nup107-160 complex, proving that the effect of depletion was specific to the removal of Nup107 and its partner proteins. These in vitro data strongly support the conclusion that the effect of partial depletion of Nup133 or Nup107 on NPC assembly seen in our in vivo experiments is both direct and specific.

In the in vitro complementation experiments, a mixture of the eluates from both Nup98 and Nup153 affinity columns was more active in complementation than either eluate alone. This might be trivial, since the eluted Nup107-160 complex was still associated with the Nup98 or Nup153-derived fusion protein when added to the extract. Each of these proteins might interfere to some extent with a distinct function of the Nup107-160 complex, such that a mixture has greater activity than either alone. Alternatively, it might mean that there are two functionally distinct forms of the complex that have different roles in NPC assembly.

A Model for the Function of the Nup107-160 Complex

The data presented support a model for the function of the Nup107-160 complex during postmitotic NE/NPC assembly (Figure 7C). The complex binds to chromatin at a very early stage in nuclear reassembly. Membrane vesicles that will give rise to the NE can still bind to chromatin and fuse into a closed NE in the absence of the complex. The group of nucleoporins recognized by mAb414 associates weakly with chromatin in the presence of the Nup107-160 complex, but not in its absence (Figure 7A). Stable binding of these nucleoporins requires both the Nup107-160 complex and the addition of membranes. Binding to chromatin of the mAb414 antigens, but not of Nup107-160 complex, is blocked by BAPTA. The stable interaction of the mAb414 antigens with the chromatin is in turn necessary for their assembly into NPCs in the growing NE. The model, and our data, therefore suggests that a critical step in NPC assembly is the formation of a "pre-NPC" by recruitment of soluble nucleoporins to the surface of chromatin in a Nup107-160 complex dependent manner. We therefore suggest, as did Sheehan et al. (1988), that postmitotic NPC assembly initiates on chromatin, rather than on the

membranes that give rise to the NE. Several detailed EM analyses of nuclear assembly in vitro or in vivo have been published. Although there is by no means agreement on the order of assembly events between these studies, at least four (Comings and Okada, 1970; Goldberg et al., 1992; Maul, 1977; Sheehan et al., 1988) provided evidence for the association of NPC-like structures with chromatin prior to NPC insertion into the NE. We suggest that the structures seen in these studies would contain, and be formed on, a Nup107-160 complex template. Nevertheless, in order to be incorporated into the NE, the pre-NPCs containing the Nup107-160 complex presumably need to make a direct or indirect interaction with one or more integral membrane proteins present in the NE vesicle fraction. The two vertebrate integral membrane nucleoporins, gp210 and POM121, are obvious candidates. Many models of NPC formation have proposed that the process would begin by recruitment of soluble nucleoporins to vesicles or preformed membranes containing integral pore membrane proteins (e.g., Drummond and Wilson, 2002; Marelli et al., 2001, and references therein), i.e., the opposite order of events to that in our model. Indeed, the absence of chromatin or any other obvious template underlying AL suggests that the NPC-like structures present in these membrane stacks are most likely recruited via binding to membrane components. Nevertheless, the fact that the Nup107-160 complex is recruited early to chromatin, and that NPC assembly does not take place in the absence of this recruitment, suggests a critical role for the interaction between chromatin and the Nup107-160 complex in postmitotic NPC formation in the NE. This requirement might arise either because the insertion process requires a closed NE but has to begin from the chromatin side of the membranes (see Macaulay and Forbes, 1996; Figure 6C) or because NPC insertion has to occur simultaneously with NE membrane fusion events. Since NPC insertion clearly proceeds in the absence of a closed NE (Goldberg et al., 1992, 1997; Wiese et al., 1997; Hetzer et al., 2001), we favor the latter possibility and represent it in the model (Figure 7B).

A final question to discuss is whether the function we propose for the Nup107-160 complex is directly related to the phenotypes observed in *S. cerevisiae* strains mutant in components of the equivalent Nup84 complex. These phenotypes include several types of defect, both in NE organization and in NPC distribution within the NPC (Doye and Hurt, 1997). It may indeed be, as has been proposed (e.g., Lutzmann et al., 2002), that these phenotypes are related to defective NPC assembly or insertion into the NE. However, it is also possible that NPC formation in a NE that is reassembling after complete mitotic breakdown is a different process from NPC insertion into a preformed NE. In the latter case, it is possible that preexisting pores in the NE could act as a template, or at least a location, for new NPC formation. Alternatively, preexisting NPCs might be necessary to allow factors required for NPC assembly to gain access to the INM via nuclear import. These factors might include components of the Nup107-160 complex. Assembly of NPCs into an existing NE is the norm for organisms such as yeasts, that undergo a closed mitosis, but also occurs during interphase in metazoan cells. Whether the vertebrate Nup107-160 complex plays a similar role during NPC assembly into an NPC-containing NE as it does during de novo postmitotic NE assembly remains to be determined.

Experimental Procedures

siRNA Experiments

The siRNA duplexes used for silencing of Nup133 (GUCGAUGAC CAGCUGACCA), Nup107 (GAGGAAAGUGUAUUCGCAG) and a control siRNA (AAGGCCGAGATCCGGCACTTGTT) were purchased from Dharmacon Research, Inc. HeLa cells were transfected using either oligofectamine (Figures 1 and 2C; Elbashir et al., 2001) or calcium phosphate precipitation (Figures 2A and 2B; Jordan et al., 1996) with 480 and 240 nM of siRNA, respectively.

Antibodies

The antibodies used were: rabbit polyclonal antibodies against human Nup133 and Nup107 (Belgareh et al., 2001), Nup96 (Fontoura et al., 1999), Nup98 (Wu et al., 2001), Nup93 (Grandi et al., 1997), Tpr (Kuznetsov et al., 2002), lamin A/C (Chaudhary and Courvalin, 1993), *Xenopus* Lamin LIII S49 (Dabauvalle et al., 1990); monoclonal antibodies mAb414 (BabCo), anti-Nup153 SA1 (Bodoor et al., 1999), and anti-SC-35 (Sigma) and autoimmune gp210 serum (Courvalin et al., 1990). Secondary antibodies were from Jackson ImmunoResearch Laboratories, Inc. or Molecular Probes.

To generate specific antibodies against *Xenopus* Nup107 (anti-Nup107), amino acids 76–171 of rat Nup107 were expressed as a His6-tagged fusion protein in pQE30 (Qiagen) in BL21[pRep4] and purified according to the manufacturers specifications. Antibodies were raised in rabbits and affinity purified. To generate a resin for the depletion from *Xenopus* egg extracts, saturating amounts of antibody were bound to Protein A Sepharose (Pharmacia) and cross-linked with 10 mM dimethylpimelimidate (Sigma).

Immunofluorescence, FISH, and EM on HeLa Cells

Immunofluorescence on HeLa cells was as described (Belgareh et al., 2001). For FISH experiments, cells processed for IF analysis were refixed for 5 min in 3% paraformaldehyde, equilibrated in 2× SSPE, prehybridized 10 min in 2× SSPE, 15% formamide, hybridized at 37°C for 2 hr with cyanine 3-oligo $(dT)_{45}$ at 50 ng/ml in 15% formamide, 2× SSPE, 1 mg/ml tRNA, and 10% dextran sulfate, then washed 20 min in 15% formamide, 2× SSPE, and 10 min in 1× SSPE. For thin section EM, HeLa cells were fixed in 2% glutaraldehyde in cacodylate buffer, washed, postfixed in 1% osmium, dehydrated in ethanol, and embedded in Epon. Sections were contrasted with uranyl acetate and lead citrate. For HeLa cell FEISEM, samples were prepared and visualized as described (Allen et al., 1998).

Nuclear Assembly and Related Methods

Fractionated egg extract preparation, immunodepletion, nuclear assembly, and FEISEM analysis were as described (Walther et al., 2001) except that nuclear assembly reactions were 20 μl. For add-back experiments, 3 μl of eluate fractions from the TAP-CAN/Nup214, TAP-Nup153, and TAP–Nup98 fusions, or of a mixture of these fractions, was added. Membranes were stained with DiOC18 or $DiIC_6$ as described (Hetzer et al., 2000) and observed live or in fixed samples. Nuclear import reactions using GFP-NLS (a gift of M. Fornerod, Netherlands Cancer Institute, Amsterdam) and BSA-SLN (Palacios et al., 1997) as a control were as described (Walther et al., 2002).

For Figure 3, incubation was with Nup133 antibody then secondary Alexa 546-coupled goat anti-rabbit IgG. After quenching this reaction with nonimmune IgG, biotinylated Nup107 antibody, and mAb414 were added. mAb414 was counterstained with Alexa 633-coupled goat anti-mouse IgG and Nup107 with streptavidin coupled to FITC. All secondary reagents were from Molecular Probes.

Purification of the Nup107 Complex from *Xenopus* Egg Extracts

To generate affinity chromatography resins, fragments of the nucleoporins Nup98 (aa531–716), Nup153 (aa210–338), and Nup214 (aa692–782) were fused to C-terminal histidine (6) and TAP tags (Rigaut et al., 1999) expressed in *E. coli*, and purified on Ni-NTA

agarose (Qiagen). For purification of the Nup107 complex, *Xenopus* egg extract was diluted to 10 mg/ml total protein and 250 mM KCl in S250 buffer (20 mM HEPES [pH 7.5], 250 mM KCl, 250 mM sucrose, 2.5 mM $MgCl_2$, and 1 mM DTT) and spun for 1 hr at 200,000 g in a Beckman SW55Ti. The supernatant was filtered and 4 ml were incubated at 4°C for 1 hr with 100 μl IgG Sepharose (Pharmacia) to which saturating amounts of one of the nucleoporin-TAP fragments was bound. The beads were washed at least 4 times with excess S250 buffer and the fragments were cleaved at 16°C for 1.5 hr by TEV protease in S250 buffer plus 0.1 mg/ml BSA. The supernatant was dialyzed against 20 mM HEPES, [pH 7.5], 50 mM KCL, 250 mM sucrose, 2.5 mM $MgCl_2$, 1 mM DTT, 20% glycerol, and 20% PEG20000, aliquoted, snap-frozen, and stored at −80°C. The different reactions were separated by SDS-PAGE (8%) and analyzed by Western blotting or mass spectrometry. Mass spectrometry was as described (Shevchenko et al., 1997, 1996). After extraction from the gel, the peptide mixture was desalted and directly eluted into the spraying capillary. Tryptic peptides were sequenced by nanoelectrospray tandem mass spectrometry on a Q-TOF1 instrument (Micromass, Manchester, United Kingdom). The product ion spectra obtained were interpreted manually. Proteins were identified by homology searching against a nonredundant database using BLAST.

Acknowledgments

We thank B. Fontoura, J. van Deursen, E. Hurt, V. Cordes, J.C. Courvalin, G. Krohne, and B. Burke for their generous gifts of antibodies; Franck Perez, Clément Nizak and Nathalie Delgehyr for help with siRNA; Brigitte David-Watine for advice on FISH; Danièle Tenza and the "Service de Microscopie Electronique, IFR BI, CNRS, Paris VI" for help with thin section EM; Maarten Fornerod for help with immunodepletion; and Wolfram Antonin and Peter Askjaer for reagents and experimental help. We thank the members of our laboratories as well as Jan Ellenberg and Maarten Fornerod for comments on the manuscript. This work was supported by EMBL and the Louis Jeantet prize for Medicine (to I.W.M.), CNRS, the Institut Curie, and the Association pour la Recherche contre le Cancer (to V.D.).

Received: November 25, 2002
Revised: February 19, 2003
Accepted: February 19, 2003
Published: April 17, 2003

References

Allen, T.D., Rutherford, S.A., Bennion, G.R., Wiese, C., Reipert, S., Kiseleva, E., and Goldberg, M.W. (1998). Three-dimensional surface structure analysis of the nucleus. In Nuclear Structure and Function, M. Berrios, ed. (San Diego, CA: Academic Press), pp. 125–138.

Allen, N.P., Huang, L., Burlingame, A., and Rexach, M. (2001). Proteomic analysis of nucleoporin interacting proteins. J. Biol. Chem. *276*, 29268–29274.

Bagley, S., Goldberg, M.W., Cronshaw, J.M., Rutherford, S., and Allen, T.D. (2000). The nuclear pore complex. J. Cell Sci. *113*, 3885–3886.

Belgareh, N., Rabut, G., Bai, S.W., van Overbeek, M., Beaudouin, J., Daigle, N., Zatsepina, O.V., Pasteau, F., Labas, V., Fromont-Racine, M., et al. (2001). An evolutionarily conserved NPC subcomplex, which redistributes in part to kinetochores in mammalian cells. J. Cell Biol. *154*, 1147–1160.

Bodoor, K., Shaikh, S., Salina, D., Raharjo, W.H., Bastos, R., Lohka, M., and Burke, B. (1999). Sequential recruitment of NPC proteins to the nuclear periphery at the end of mitosis. J. Cell Sci. *112*, 2253–2264.

Chaudhary, N., and Courvalin, J. (1993). Stepwise reassembly of the nuclear envelope at the end of mitosis. J. Cell Biol. *122*, 295–306.

Comings, D.E., and Okada, T.A. (1970). Association of chromatin fibers with the annuli of the nuclear membrane. Exp. Cell Res. *62*, 293–302.

Conti, E., and Izaurralde, E. (2001). Nucleocytoplasmic transport enters the atomic age. Curr. Opin. Cell Biol. *13*, 310–319.

Courvalin, J.C., Lassoued, K., Bartnik, E., Blobel, G., and Wozniak, R.W. (1990). The 210-kD nuclear envelope polypeptide recognized by human autoantibodies in primary biliary cirrhosis is the major glycoprotein of the nuclear pore. J. Clin. Invest. *86*, 279–285.

Cronshaw, J.M., Krutchinsky, A.N., Zhang, W., Chait, B.T., and Matunis, M.J. (2002). Proteomic analysis of the mammalian nuclear pore complex. J. Cell Biol. *158*, 915–927.

Dabauvalle, M.C., Loos, K., and Scheer, U. (1990). Identification of a soluble precursor complex essential for nuclear pore assembly in vitro. Chromosoma *100*, 56–66.

Daigle, N., Beaudouin, J., Hartnell, L., Imreh, G., Hallberg, E., Lippincott-Schwartz, J., and Ellenberg, J. (2001). Nuclear pore complexes form immobile networks and have a very low turnover in live mammalian cells. J. Cell Biol. *154*, 71–84.

Davis, L.I., and Blobel, G. (1986). Identification and characterization of a nuclear pore complex protein. Cell *45*, 699–709.

Doye, V., and Hurt, E. (1997). From nucleoporins to nuclear pore complexes. Curr. Opin. Cell Biol. *9*, 401–411.

Drummond, S.P., and Wilson, K.L. (2002). Interference with the cytoplasmic tail of gp210 disrupts "close apposition" of nuclear membranes and blocks nuclear pore dilation. J. Cell Biol. *158*, 53–62.

Elbashir, S., Harborth, J., Lendeckel, W., Yalcin, A., Weber, K., and Tuschl, T. (2001). Duplexes of 21-nucleotide RNAs mediate RNA interference in cultured mammalian cells. Nature *411*, 494–498.

Finlay, D.R., and Forbes, D.J. (1990). Reconstitution of biochemically altered nuclear pores: transport can be eliminated and restored. Cell *60*, 17–29.

Finlay, D.R., Meier, E., Bradley, P., Horecka, J., and Forbes, D.J. (1991). A complex of nuclear pore proteins required for pore function. J. Cell Biol. *114*, 169–183.

Fontoura, B.M., Blobel, G., and Matunis, M.J. (1999). A conserved biogenesis pathway for nucleoporins: proteolytic processing of a 186-kilodalton precursor generates Nup98 and the novel nucleoporin, Nup96. J. Cell Biol. *144*, 1097–1112.

Forbes, D.J., Kirschner, M.W., and Newport, J.W. (1983). Spontaneous formation of nucleus-like structures around bacteriophage DNA microinjected into *Xenopus* eggs. Cell *34*, 13–23.

Goldberg, M.W., Blow, J.J., and Allen, T.D. (1992). The use of field emission in-lens scanning electron microscopy to study the steps of assembly of the nuclear envelope in vitro. J. Struct. Biol. *108*, 257–268.

Goldberg, M.W., Wiese, C., Allen, T.D., and Wilson, K.L. (1997). Dimples, pores, star-rings, and thin rings on growing nuclear envelopes: evidence for structural intermediates in nuclear pore complex assembly. J. Cell Sci. *110*, 409–420.

Görlich, D., and Kutay, U. (1999). Transport between the cell nucleus and the cytoplasm. Annu. Rev. Cell Dev. Biol. *15*, 607–660.

Grandi, P., Dang, T., Pane, N., Shevchenko, A., Mann, M., Forbes, D., and Hurt, E. (1997). Nup93, a vertebrate homologue of yeast Nic96p, forms a complex with a novel 205-kDa protein and is required for correct nuclear pore assembly. Mol. Biol. Cell *8*, 2017–2038.

Haraguchi, T., Koujin, T., Hayakawa, T., Kaneda, T., Tsutsumi, C., Imamoto, N., Akazawa, C., Sukegawa, J., Yoneda, Y., and Hiraoka, Y. (2000). Live fluorescence imaging reveals early recruitment of emerin, LBR, RanBP2, and Nup153 to reforming functional nuclear envelopes. J. Cell Sci. *113*, 779–794.

Hetzer, M., Bilbao-Cortes, D., Walther, T.C., Gruss, O.J., and Mattaj, I.W. (2000). GTP hydrolysis by Ran is required for nuclear envelope assembly. Mol. Cell *5*, 1013–1024.

Hetzer, M., Meyer, H.H., Walther, T.C., Bilbao-Cortes, D., Warren, G., and Mattaj, I.W. (2001). Distinct AAA-ATPase p97 complexes function in discrete steps of nuclear assembly. Nat. Cell Biol. *3*, 1086–1091.

Imreh, G., and Hallberg, E. (2000). An integral membrane protein from the nuclear pore complex is also present in the annulate lamellae: implications for annulate lamella formation. Exp. Cell Res. *259*, 180–190.

Jordan, M., Schallhorn, A., and Wurm, F.M. (1996). Transfecting

mammalian cells: optimization of critical parameters affecting calcium-phosphate precipitate formation. Nucleic Acids Res. *24*, 596–601.

Kuznetsov, N., Sandblad, L., Hase, M., Hunziker, A., Hergt, M., and Cordes, V. (2002). The evolutionarily conserved single-copy gene for murine Tpr encodes one prevalent isoform in somatic cells and lacks paralogs in higher eukaryotes. Chromosoma *111*, 236–255.

Lohka, M.J., and Masui, Y. (1983). Formation in vitro of sperm pronuclei and mitotic chromosomes induced by amphibian ooplasmic components. Science *220*, 719–721.

Lutzmann, M., Kunze, R., Buerer, A., Aebi, U., and Hurt, E. (2002). Modular self-assembly of a Y-shaped multiprotein complex from seven nucleoporins. EMBO J. *21*, 387–397.

Macaulay, C., and Forbes, D.J. (1996). Assembly of the nuclear pore: biochemically distinct steps revealed with NEM, GTPγS, and BAPTA. J. Cell Biol. *132*, 5–20.

Marelli, M., Lusk, C.P., Chan, H., Aitchison, J.D., and Wozniak, R.W. (2001). A link between the synthesis of nucleoporins and the biogenesis of the nuclear envelope. J. Cell Biol. *153*, 709–724.

Mattaj, I.W., and Englmeier, L. (1998). Nucleocytoplasmic transport: the soluble phase. Annu. Rev. Biochem. *67*, 265–306.

Maul, G.G. (1977). Nuclear pore complexes. Elimination and reconstruction during mitosis. J. Cell Biol. *74*, 492–500.

Newport, J. (1987). Nuclear reconstitution in vitro: stages of assembly around protein-free DNA. Cell *48*, 205–217.

Ohno, M., Fornerod, M., and Mattaj, I.W. (1998). Nucleocytoplasmic transport: the last 200 nanometers. Cell *92*, 327–336.

Palacios, I., Hetzer, M., Adam, S.A., and Mattaj, I.W. (1997). Nuclear import of UsnRNPs requires importin β. EMBO J. *16*, 6783–6792.

Powers, M.A., Forbes, D.J., Dahlberg, J.E., and Lund, E. (1997). The vertebrate GLFG nucleoporin, Nup98, is an essential component of multiple RNA export pathways. J. Cell Biol. *136*, 241–250.

Radu, A., Blobel, G., and Wozniak, R.W. (1994). Nup107 is a novel nuclear pore complex protein that contains a leucine zipper. J. Biol. Chem. *269*, 17600–17605.

Rigaut, G., Shevchenko, A., Rutz, B., Wilm, M., Mann, M., and Seraphin, B. (1999). A generic protein purification method for protein complex characterization and proteome exploration. Nat. Biotechnol. *17*, 1030–1032.

Rout, M.P., Aitchison, J.D., Suprapto, A., Hjertaas, K., Zhao, Y., and Chait, B.T. (2000). The yeast nuclear pore complex: composition, architecture, and transport mechanism. J. Cell Biol. *148*, 635–651.

Sheehan, M.A., Mills, A.D., Sleeman, A.M., Laskey, R.A., and Blow, J.J. (1988). Steps in the assembly of replication-competent nuclei in a cell-free system from *Xenopus* eggs. J. Cell Biol. *106*, 1–12.

Shevchenko, A., Wilm, M., Vorm, O., and Mann, M. (1996). Mass spectrometric sequencing of proteins silver-stained polyacrylamide gels. Anal. Chem. *68*, 850–858.

Shevchenko, A., Chernushevich, I., Ens, W., Standing, K.G., Thomson, B., Wilm, M., and Mann, M. (1997). Rapid 'de novo' peptide sequencing by a combination of nanoelectrospray, isotopic labeling and a quadrupole/time-of-flight mass spectrometer. Rapid Commun. Mass Spectrom. *11*, 1015–1024.

Siniossoglou, S., Wimmer, C., Rieger, M., Doye, V., Tekotte, H., Weise, C., Emig, S., Segref, A., and Hurt, E.C. (1996). A novel complex of nucleoporins, which includes Sec13p and a Sec13p homolog, is essential for normal nuclear pores. Cell *84*, 265–275.

Siniossoglou, S., Lutzmann, M., Santos-Rosa, H., Leonard, K., Mueller, S., Aebi, U., and Hurt, E. (2000). Structure and assembly of the Nup84p complex. J. Cell Biol. *149*, 41–54.

Stoffler, D., Fahrenkrog, B., and Aebi, U. (1999). The nuclear pore complex: from molecular architecture to functional dynamics. Curr. Opin. Cell Biol. *11*, 391–401.

Vasu, S.K., and Forbes, D.J. (2001). Nuclear pores and nuclear assembly. Curr. Opin. Cell Biol. *13*, 363–375.

Vasu, S., Shah, S., Orjalo, A., Park, M., Fischer, W.H., and Forbes, D.J. (2001). Novel vertebrate nucleoporins Nup133 and Nup160 play a role in mRNA export. J. Cell Biol. *155*, 339–354.

Walther, T.C., Fornerod, M., Pickersgill, H., Goldberg, M., Allen, T.D., and Mattaj, I.W. (2001). The nucleoporin Nup153 is required for nuclear pore basket formation, nuclear pore complex anchoring and import of a subset of nuclear proteins. EMBO J. *20*, 5703–5714.

Walther, T.C., Pickersgill, H.S., Cordes, V.C., Goldberg, M.W., Allen, T.D., Mattaj, I.W., and Fornerod, M. (2002). The cytoplasmic filaments of the nuclear pore complex are dispensable for selective nuclear protein import. J. Cell Biol. *158*, 63–77.

Wiese, C., Goldberg, M.W., Allen, T.D., and Wilson, K.L. (1997). Nuclear envelope assembly in *Xenopus* extracts visualized by scanning EM reveals a transport-dependent 'envelope smoothing' event. J. Cell Sci. *110*, 1489–1502.

Wu, X., Kasper, L.H., Mantcheva, R.T., Mantchev, G.T., Springett, M.J., and van Deursen, J.M. (2001). Disruption of the FG nucleoporin NUP98 causes selective changes in nuclear pore complex stoichiometry and function. Proc. Natl. Acad. Sci. USA *98*, 3191–3196.